

Verification of Limit Equilibrium Methods (LEM)

Ching-Chuan Huang

Professor Emeritus
Department of Civil Engineering,
National Cheng Kung University, Tainan, Taiwan
Email: samhcc@mail.ncku.edu.tw
2025/03/13

INTRODUCTION

SLOPE-ffdm 2.0 is a window-based computer program for evaluating stability and predicting possible displacements of natural and man-made slopes. The program features the following two functions: (1) a basic function of slope stability analysis using various limit equilibrium methods, including the Fellinius', the Bishop's, the Mogenstern-Price method, the Spencer's and the Janbu's methods, and (2) an advanced function of calculating slope displacements using Force-equilibrium-based Finite Displacement Method (FFDM) which is described in Series 1 and Series 4- 7. This series of reports focuses on the verification of the above-mentioned limit equilibrium methods of slice using some well-documented case studies.

Results of the comparative study in this series of report show that values of safety factor (F_s) for a specific failure surface generated by SLOPE-ffdm 2.0 deviated from those reported in the literature within an acceptable range of 3%. The values of F_s obtained for the slopes using trial-and-error search of critical surfaces are generally smaller than those reported in the literature. These results confirm the accuracy and precision of the formulation and computer algorithms in SLOPE-ffdm 2.0.

3.1 VERIFICATION CASE STUDY NO. 1

Input file name:

verification_type-1_Duncan&Wright_Fig.7.6_input.txt
verification_type-2_Duncan&Wright_Fig.7.6_input.txt
verification_type-3_Duncan&Wright_Fig.7.6_input.txt

Output file name:

verification_type-1_Duncan&Wright_Fig.7.6_output.txt
verification_type-2_Duncan&Wright_Fig.7.6_output.txt
verification_type-3_Duncan&Wright_Fig.7.6_output.txt

This is a vertical cut of a varved clay with assumed tension crack depths from 0 to 4 ft (Figure 7.6 in Duncan and Wright, 2005). Type-1 analysis of SLOPE-ffdm 2.0 with a grid of rotation centers is shown in Fig. 3.1.1. A total of 1,349 trial-and-error circular surfaces is used. In the input data file, five events with various tension crack depths are included. Fig. 3.1.2 shows the graphics of the critical surface found in Fellenius', Bishop's and Spencer's methods. In the case of $\phi = 0$ analysis, these three methods generate identical values of F_s . Comparisons between the reported values of F_s and those obtained in Type-1 analysis are shown in Table 3.1.1. Values of F_s obtained here are comparable to those reported in the literature.

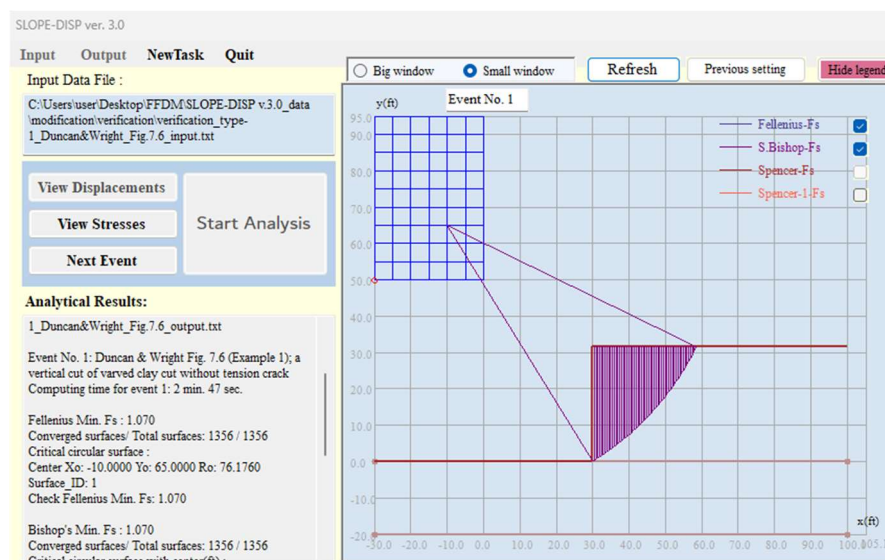


Figure 3.1.1 Graphics for the result of analysis for event 1
without a tension crack

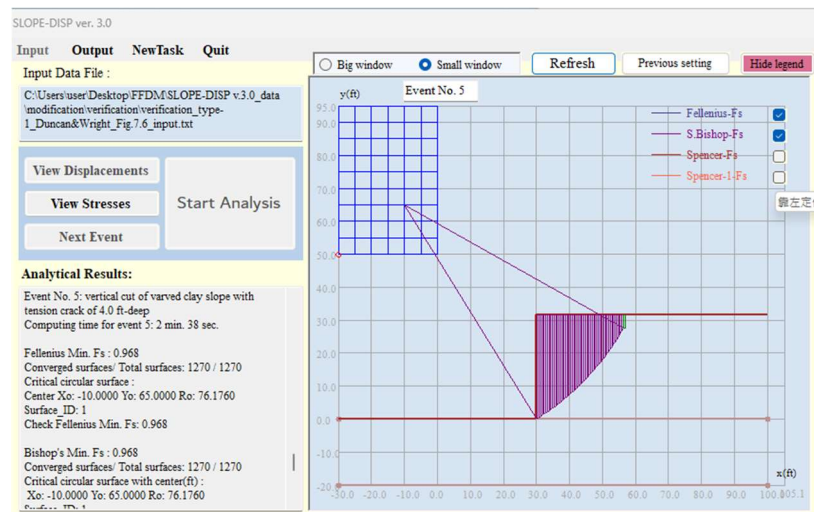


Figure 3.1.2 Graphics for the result of analysis for event 5 with a 4.0 ft-deep tension crack

Table 3.1.1 Safety factors calculated by Type-1 analysis and those reported by Duncan and Wright (2005)

Depth of tension crack (ft)	F_s by Duncan and Wright (2005)	F_s by SLOPE-ffdm 2.0
0	1.06	1.070
1	1.04	1.043
2	1.01	1.017
3	0.99	0.992
4	0.96	0.968

To examine the integrity of SLOPE-ffdm 2.0, Type-2 (passing-through-a-point circular-surface analysis) and Type-3 (one-circular-surface analysis) are also performed. In the Type-2 analysis, the grid of rotation center is the same with that in Type-1 analysis and the toe of the slope (30.0, 0.0) is the point of passing-through. They generated values of F_s slightly smaller than those shown in Table 3.1.1, revealing the effectiveness of Type-2 analysis, in the sense that a passing-through-slope-toe analysis can provide more accurate results in the case of a vertical cut. Note that two soil strata are used in the analysis: soil layer No. 1 (the topmost layer) is with an undrained shear strength of $c_u = 1050$ psf (pound/ft²), $\phi = 0^\circ$, the layer No. 2 (the bottom layer) is assigned with high strengths of $c_u = 3000$ psf, $\phi = 40^\circ$ to avoid a below-toe failure (or deep failure). The output minimum values of F_s for Type-1, Type-2 and Type-3 analyses are summarized in Table 3.1.2. Also note that in Type-3 analysis which is a one-circle analysis, the input values of rotation center and radius are the critical ones obtained in Type-2 analysis.

Therefore, identical values of F_s are obtained for Type-2 and Type-3 analyses as shown in Table 3.1.2.

Table 3.1.2 F_s calculated by Type-1, Type-2 and Type-3 analyses

Depth of tension crack (ft)	F_s by Type-1	F_s by Type-2	F_s by Type-3
0	1.070	1.064	1.064
1	1.043	1.037	1.037
2	1.017	1.011	1.011
3	0.992	0.986	0.986
4	0.968	0.961	0.961

3.2 VERIFICATION CASE STUDY NO. 2

Input and output files for case study No. 2:

Input file name: verification_type-1_Duncan&Wright_Fig.7.7_input.txt
Output file name: verification_type-1_Duncan&Wright_Fig.7.7_output.txt

This case study is an underwater slope in San Francisco Bay mud reported by Duncan and Buchignani (1973). A part of the slope failed during construction. It was reported that F_s calculated using Spencer's method was 1.17 (with no detail of critical surface). Table 3.2.1 summarizes values of F_s given by Type-1 analysis in SLOPE-ffdm 2.0. All methods (Fellenius, Bishop, and Spencer) give $F_s = 1.056$ based on the reported undrained strength profile: a saturated unit weight of $\gamma_{sat} = 100.4$ pcf with an undrained strength at the mud surface, $c_{u0} = 98.2$ psf and an increasing rate of $\Delta c_u / \Delta z = 10.145$ psf /ft. For the debris dike, $\gamma_{sat} = 87.4$ pcf and a uniform undrained strength of $c_u = 800$ psf. The critical failure surface obtained in a trial-and-error search is shown in Fig. 3.2.1. It is considered that the discrepancy between the reported $F_s = 1.17$ and $F_s = 1.056$ obtained here reflects not only the improvement of digital technology but also the intensity of the trial-and-error surfaces (a total number of 734) used here. The results of $F_s = 1.056$ well complies with the observed failure for the marginally stable slope during construction.

Table 3.2.1 also highlights an important feature of the computer program, i.e., the use of submerged soil unit weight (using 'water table' command with ID= 3) and total unit weight associated with hydrostatic water pressures (using 'water table' command with ID= 4) resulted in identical failure surface (Figs. 3.2.1 and Fig. 3.2.2) and values of F_s (Table 1.2.1). This ensures that the effect of porewater pressure is accurately accounted for in the computations.

Table 3.2.1 F_s based on different considerations of porewater pressures

	F_s using Submerged unit weight (Event 1)	F_s using Hydrostatic pressure (Event 2)
Type-1 analysis	1.056	1.056
Type-3 analysis	1.056	1.056

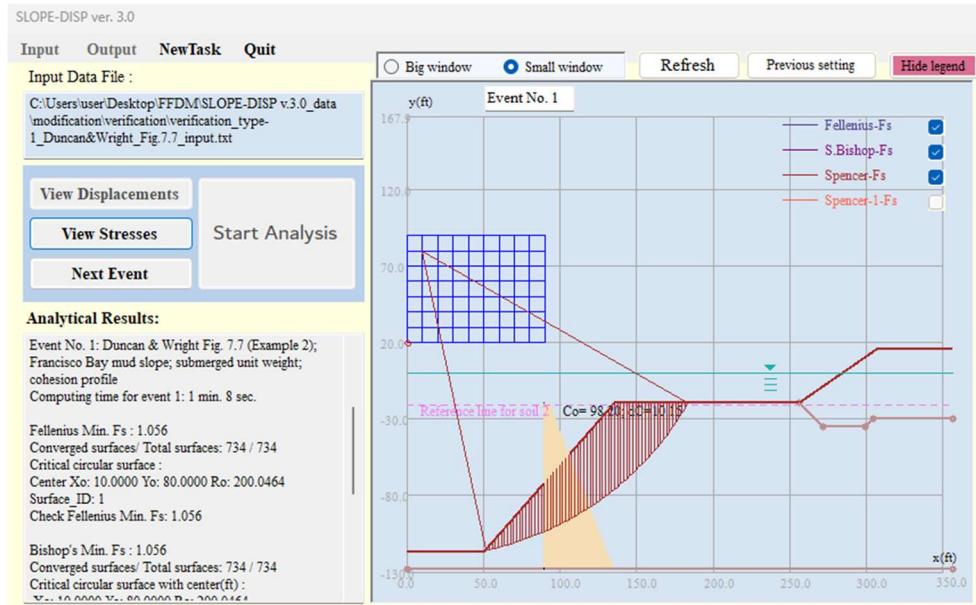


Figure 3.2.1 Critical surface found in 734 trial-and-error arcs using submerged unit weight of soils

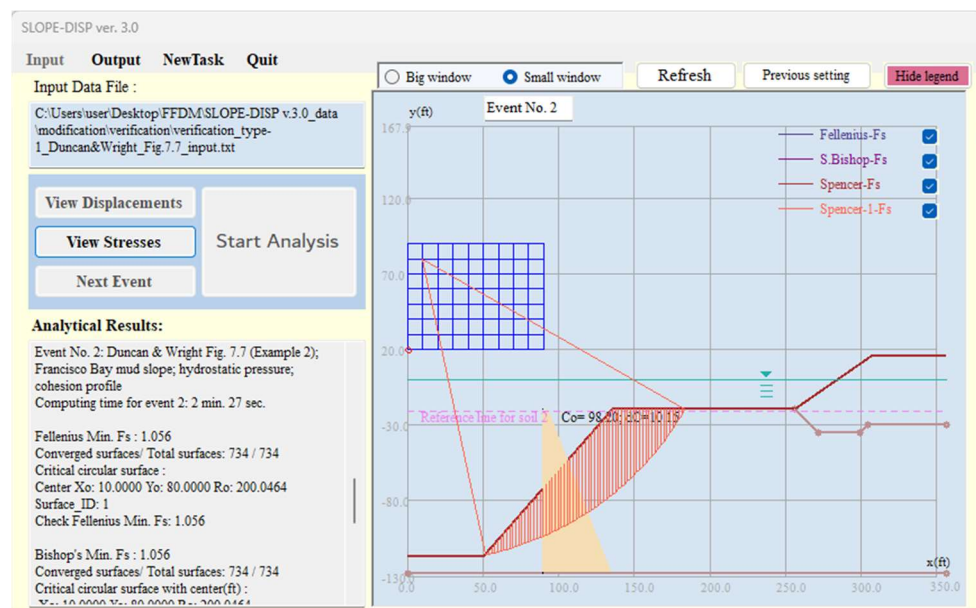


Figure 3.2.2 Critical surface found in 734 trial-and-error arcs using saturated unit weight of soils and hydrostatic porewater pressures

3.3 VERIFICATION CASE STUDY NO. 3

Input and output files for case study No. 3:

Input file name: verification_type-1_Duncan&Wright_Fig.7.9_input.txt
Input file name: verification_type-2_Duncan&Wright_Fig.7.9_input.txt
Output file name: verification_type-1_Duncan&Wright_Fig.7.9_output.txt
Output file name: verification_type-2_Duncan&Wright_Fig.7.9_output.txt

This case study was reported by Duncan and Wright (2005) for an excavated slope consisting of London clay. The slope consists of four layers of soils: layer No. 1 (top) is an embankment fill (replaced by equivalent surcharge because it is cracked to the full depth); layer No. 2 is with a uniform undrained strength $c_u = 300$ psf; layer No. 3 is with a cohesion profile of $c_{u0} = 860$ psf at top and an increasing rate of $\Delta c_u / \Delta z = 65$ psf/ft; layer No. 4 is with $c_{u0} = 2420$ psf and $\Delta c_u / \Delta z = 35$ psf/ft. Figure 3.3.1 shows the critical failure surface as a result of 2959 trial-and-error search. All methods used in the program (Fellenius, Bishop, Spencer, and Spencer-1) generated identical critical surfaces and minimum values of $F_s (= 1.714)$. This value of F_s is slightly smaller than $F_s = 1.76- 1.80$ (Table 3.3.1) reported by Duncan and Wright (2005) for about 2%- 5% which is within an acceptable range.

As summarized in Table 3.3.1, Type-2 analysis (passing-through-a-specific-point analysis) is also performed by setting the slope toe ($x = 20.0$, $y = -31.0$) as the default passing-through point. The minimum value of $F_s (= 1.708)$, regardless of various methods used) found in Type-2 analysis is slightly smaller than that in Type-1 analysis ($F_s = 1.714$). This result is comparable to that found in Case Study No. 1 which showed Type-3 analysis can be more effective in the case of a steep slope which often exhibits a passing-through-slope-toe failure.

Table 3.3.1 Comparisons of minimum values of F_s obtained in various studies.

	Duncan and Wright (2005)	Type-1 analysis; SLOPE-ffdm 2.0	Type-2 analysis; SLOPE-ffdm 2.0
F_s	1.76- 1.80	1.714	1.708

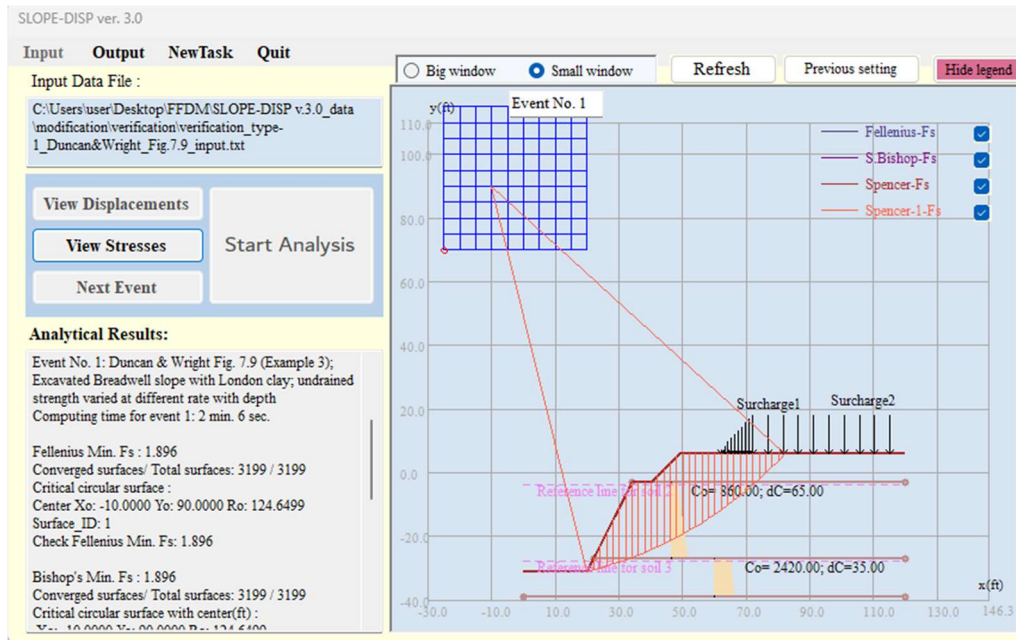


Figure 3.3.1 Critical surface for the slope consisting of London clay
(Figure 7.9 of Duncan and Wright, 2005)

3.4 VERIFICATION CASE STUDY NO. 4

Input and output files for case study No. 4:

Input file name: verification_type-1_3_Duncan&Wright_Fig.7.12_input.txt

Output file name: verification_type-1_3_Duncan&Wright_Fig.7.12_output.txt

This is a hypothetical embankment consisting of a granular material ($c=0$) resting on a saturated clay ($\phi=0$) foundation (Fig. 7.12 of Duncan and Wright, 2005). Details of the geometry of the critical circle were reported, allowing a straightforward comparative study using SLOPE-ffdm 2.0. Results of Type-1 analysis indicate that critical circles are close to (but not identical) to the one reported by Duncan and Wright (2005) as shown in Fig. 3.4.1. The minimum values of F_s found in Type-1 analysis are 0.8-1.5% smaller than the reported one as shown in Table 3.4.1. Results of Type-3 analysis for the same critical circular surface reported by Duncan and Wright (2005) generate almost identical values of F_s to the reported one as shown in Table 3.4.1.

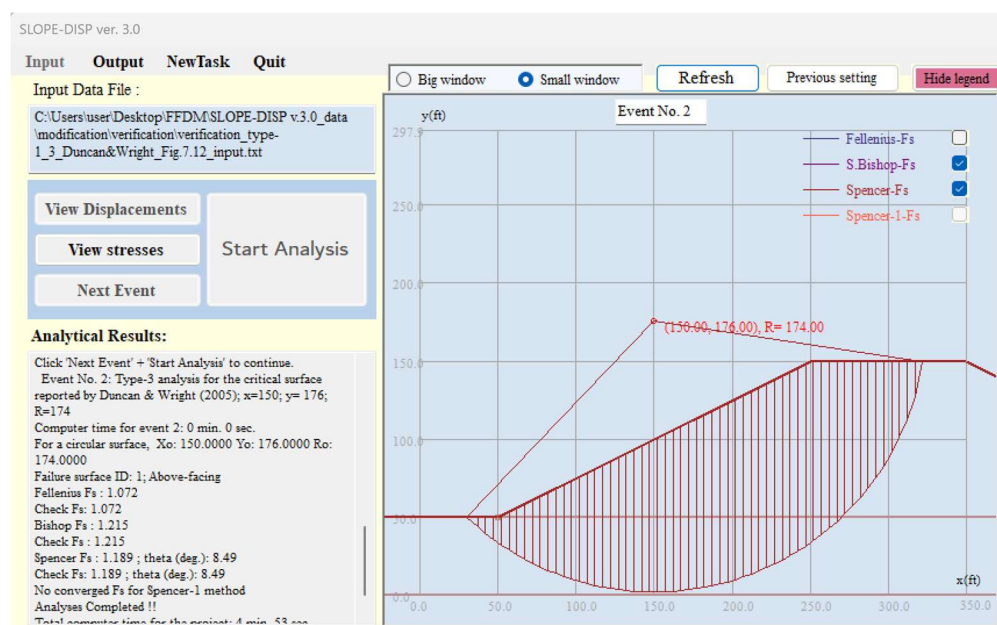


Figure 3.4.1 Type-3 analysis (Event 2 of the input data file) for the critical failure circle reported in Figure 7.12 of Duncan and Wright (2005).

Table 3.4.1 Comparisons of safety factors obtained in various studies.

	Duncan and Wright (2005)	Type-1 analysis	Type-3 analysis
Bishop's F_s	1.22	1.202	1.215
Spencer's F_s	1.19	1.180	1.189

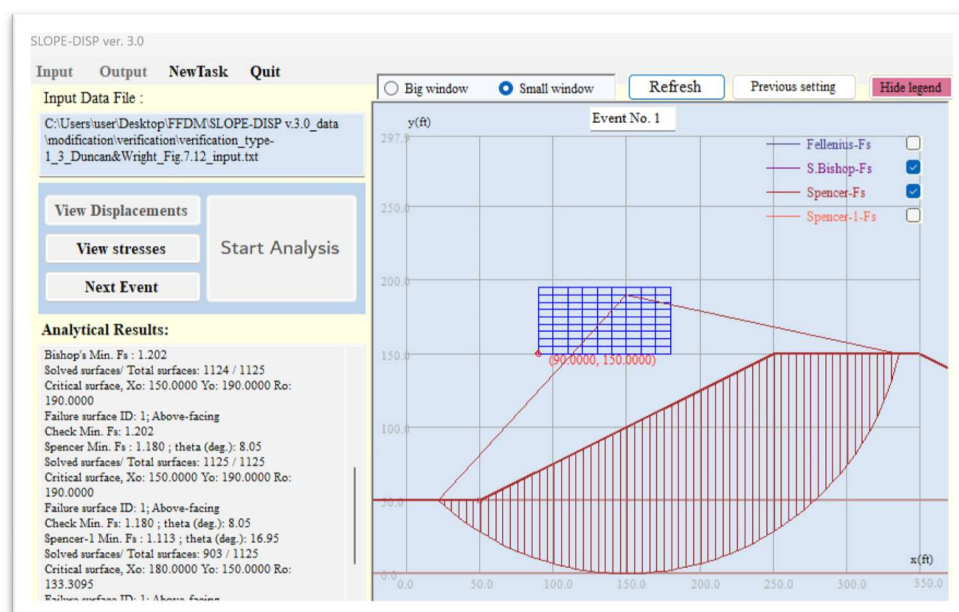


Figure 3.4.2 Critical surface found in Type-1 analysis (Event 1 of the input data file)

3.5 VERIFICATION CASE STUDY NO. 5

Input and output files for case study No. 5:

Input file name: verification_type-1_Duncan&Wright_Fig.7.14_input.txt
Output file name: verification_type-1_Duncan&Wright_Fig.7.14_output.txt

This is a study of the downstream slope stability of the Oroville dam (Fig. 7.14 of Duncan and Wright, 2005). The downstream slope is composed of rock fill which has a curved (or nonlinear) Mohr-Coulomb failure envelope. The following equation is frequently used to express the curved failure envelope for a cohesionless material:

$$\varphi = \varphi_0 - \Delta\varphi \cdot \log \frac{\sigma'_3}{p_a} \quad (3-5-1)$$

φ : internal friction angle

φ_0 : internal friction angle at confining pressures lower than p_a

p_a : atmospheric pressure

$\Delta\varphi$: rate of internal friction angle reduction per logarithmic cycle of pressure increase

σ'_3 : effective minor principal confining pressure

In limit-equilibrium-based stability analyses, values of σ'_3 along the slip surface are known and values of σ'_n are usually unknown. Based on a stress analysis using Mohr circles for the downstream shell material of Oroville Dam, the following relationship between σ'_3 and σ'_n was suggested by Duncan and Wright (2005):

$$\sigma'_3 = \frac{\sigma'_n}{b_n} \quad (3-5-2)$$

b_n is a factor between 1.5 and 1.8. Combining Eqs. (3-5-1) and (3-5-2) yields:

$$\varphi = [\varphi_0 + \log b_n \cdot \Delta\varphi] - \Delta\varphi \cdot \log \frac{\sigma'_n}{p_a} \quad (3-5-3)$$

According to Eq. 3-5-3, by adjusting input values of φ_0 as that shown in the parenthesis of the equation, various values of b_n ($= 1.0, 1.5$ and 1.8) can be considered in the analysis using SLOPE-ffdm 2.0. Using the reported values of $\varphi_0 = 51^\circ$, $\Delta\varphi = 6^\circ$ and various values of b_n ($= 1.0, 1.5$, and 1.8), results of Event 1 through Event 4 of Type-1 analyses are summarized in Table 3.5.1. Results shown in this table reveal that increasing the value of b_n from 1.5 to 1.8 influences minimum values of F_s only to a negligibly small degree. The case of $b_n = 1.0$ (Event 1) is used to investigate the

influence of assuming $\sigma'_3 = \sigma'_n$. By comparing the results of event 1 and 3, this assumption generates a less than 1% error of F_s . In general, ignoring the effect of the curved Mohr-Coulomb envelope (comparing results of Event 1 and 4), resulted in a significant overestimation of F_s for 16-17% and a shallower critical surface (comparing the critical surfaces in Figs. 3.5.1 and 3.5.2).

Table 3.5.1 Comparisons of safety factors obtained in various studies.

	Duncan and Wright (2005)	Event 1 ($\Delta\phi=6^\circ$, $b_n=1.0$)	Event 2 ($\Delta\phi=6^\circ$, $b_n=1.5$)	Event 3 ($\Delta\phi=6^\circ$, $b_n=1.8$)	Event 4 ($\Delta\phi=0^\circ$)
Bishop F_s	-	2.199	2.207	2.210	2.577
Spencer F_s	2.28	2.198	2.206	2.210	2.577

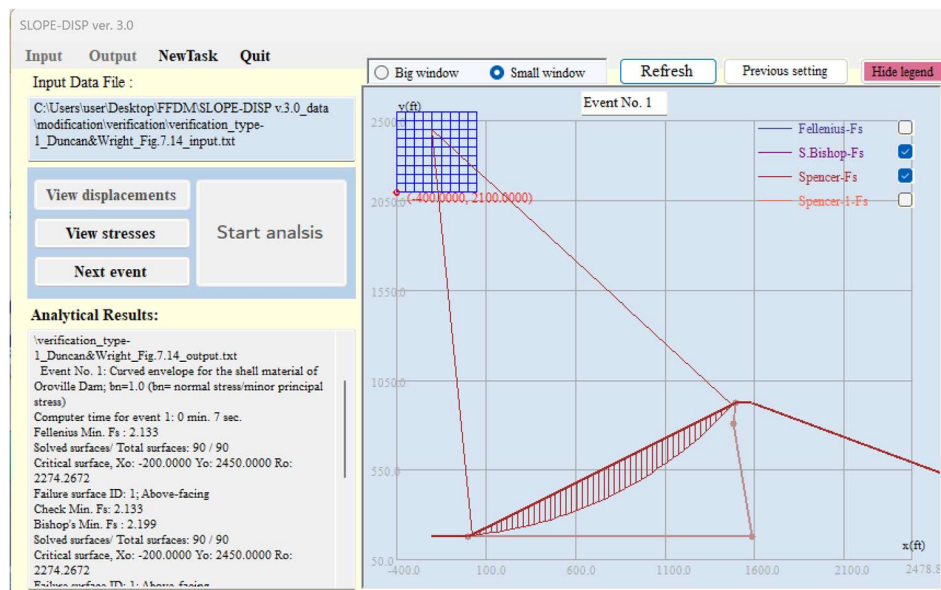


Figure 3.5.1 Critical circular surface found in Event 1 of trial-and-error analysis considering curved Mohr-Coulomb failure envelope with $\Delta\phi=6^\circ$ and $b_n=1.5$.

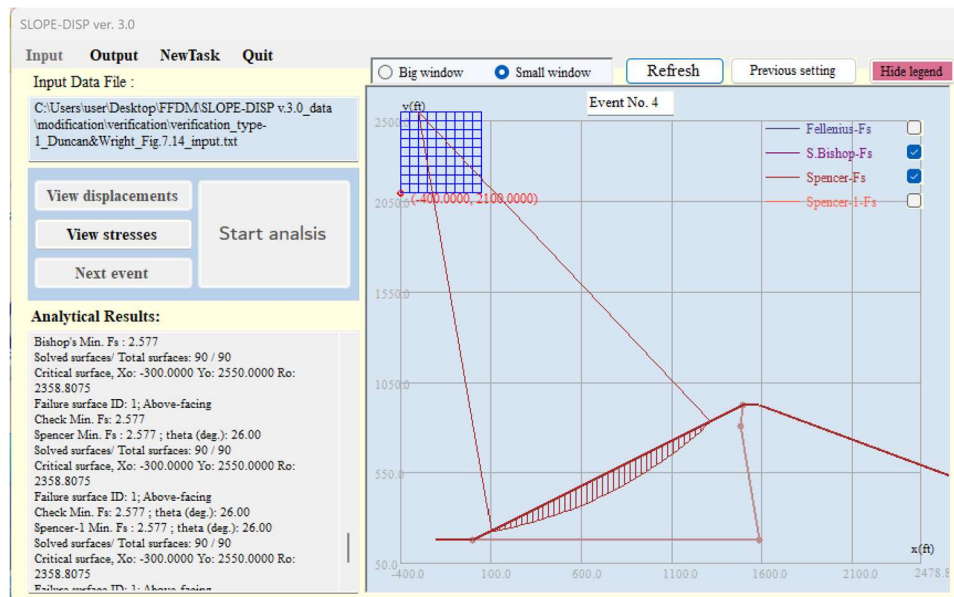


Figure 3.5.2 Critical circular surface found in Event 4 of trial-and-error analysis considering curved Mohr-Coulomb failure envelope with $\Delta\phi = 0^\circ$

3.6 VERIFICATION CASE STUDY NO. 6

Input and output files for case study No. 6:

Input file name: verification_type-1_7_Duncan&Wright_Fig.7.16_input.txt
Output file name: verification_type-1_7_Duncan&Wright_Fig.7.16_output.txt

This is a 12 m-high dike (James Bay Dike) built on multi-layer soft clays. The following two types of analysis using Spencer's procedure were reported by Duncan and Wright (2005):

- (1) Circular failure analyses: This analysis yields a minimum value of $F_s = 1.45$.
- (2) Noncircular failure analyses: This analysis yields a minimum value of $F_s = 1.17$.

In the study using SLOPE-ffdm 2.0, a Type-1 analysis (Event 1) is implemented to simulate the condition of (1). A minimum value of $F_s = 1.462$ is obtained, which is 0.8% larger than the reported value of $F_s = 1.45$. The Type-7 analysis (Event 2) encompassing a composite failure pattern is used to simulate the condition of (2). The resulted minimum value of $F_s = 1.157$ is 1.1% smaller than the reported value of $F_s = 1.17$. Comparisons of F_s obtained using various analytical procedures are summarized in Table 3.6.1. Critical failure surfaces found in Type-1 and Type-7 analyses are shown in Fig. 3.6.1 and Fig. 3.6.2, respectively. Both values of F_s and geometries of critical surfaces are comparable to those reported in the literature.

Table 3.6.1 Comparisons of F_s for James Bay dike obtained in various studies.

	Duncan and Wright (2005), F_s (Spencer's method)	SLOPE-ffdm 2.0 F_s (Spencer's method)
Critical circular surface	1.45	1.462 (Event 1: type-1 analysis)
Critical composite surface	1.17	1.157 (Event 2: type-7 analysis)

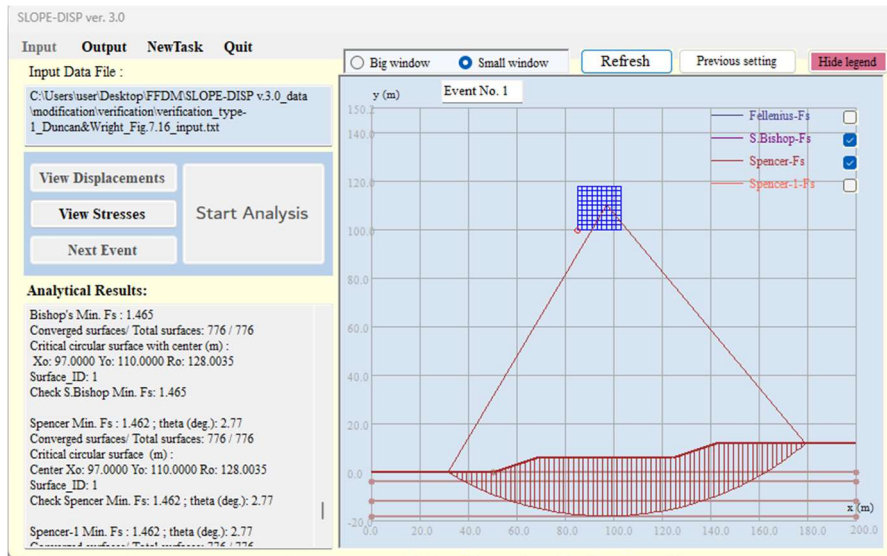


Figure 3.6.1 Critical surface obtained in Event 1 (type-1 analysis) of SLOPE-ffdm 2.0.

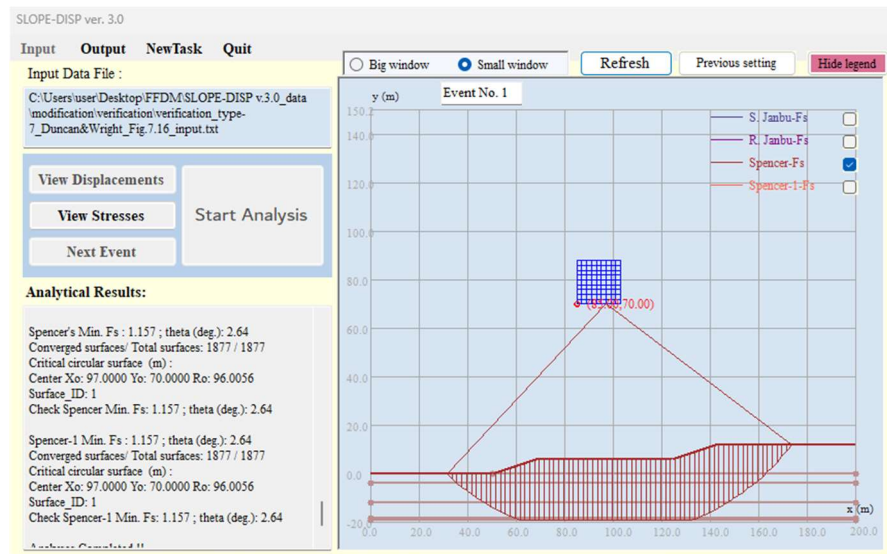


Figure 3.6.2 Critical surface obtained in Event 2 (type-7 analysis) of SLOPE-ffdm 2.0.

3.7 VERIFICATION CASE STUDY NO. 7

Input and output files for case study No. 7:

Input file name: verification_type-1_Duncan&Wright_Fig.7.19_input.txt
Output file name: verification_type-1_Duncan&Wright_Fig.7.19_output.txt

This is a 48-feet high homogeneous embankment ($c=100$ psf, $\phi'=30$, $\gamma=100$ pcf) impounds water on one side and develops a steady-state flow on the other side. The phreatic surface and the piezometric line are assumed to be the same line. The phreatic line is digitized and reproduced in Fig. 3.7.1 based on that depicted in Fig. 7.20 of Duncan and Wright (2005). The following two modes of the ‘water table’ command are used in the SLOPE-DISP stability analysis:

In Event 1 of the input data file: Mode-1 (Piezometric line) is used

In Event 2 of the input data file: Mode-5: (Phreatic surface) is used.

The values of F_s for Event 1 of Type-1 (trial-and-error circular failure analysis) of SLOPE-ffdm 2.0 with 644 trial-and-error circular surfaces are compared with those reported by Duncan and Wright (2005) in Table 3.7.1. The values of F_s obtained using Spencer’s procedure are about 7-9% lower than those reported. It is partially attributable to the error associated with the digitization of the phreatic line reported in the literature. Figures 3.7.1 and 3.7.2 indicate that close-to-toe failures dominate the stability of the slope. The location of critical failure surface confirms a common knowledge regarding the stability of slopes subjected to seepages, i.e., a saturated slope toe where a combined effect of relatively high porewater pressure and a low confining pressure may initiate a slope failure (Huang et al., 2008). It is noted that in the SLOPE-ffdm 2.0 analysis, Spencer’s and Bishop’s procedures generate identical critical failure surfaces as shown in Figs. 3.7.1 and 3.7.2.

Table 3.7.1 Comparisons of F_s obtained using different types of porewater pressures and methodologies.

	Duncan and Wright (2005) F_s (Spencer’s method)	SLOPE-ffdm 2.0 F_s (Spencer’s method)	SLOPE-ffdm 2.0 F_s (Bishop’s method)
Piezometric line (Event 1)	1.16	1.057	1.050
Phreatic surface (Event 2)	1.24	1.152	1.145

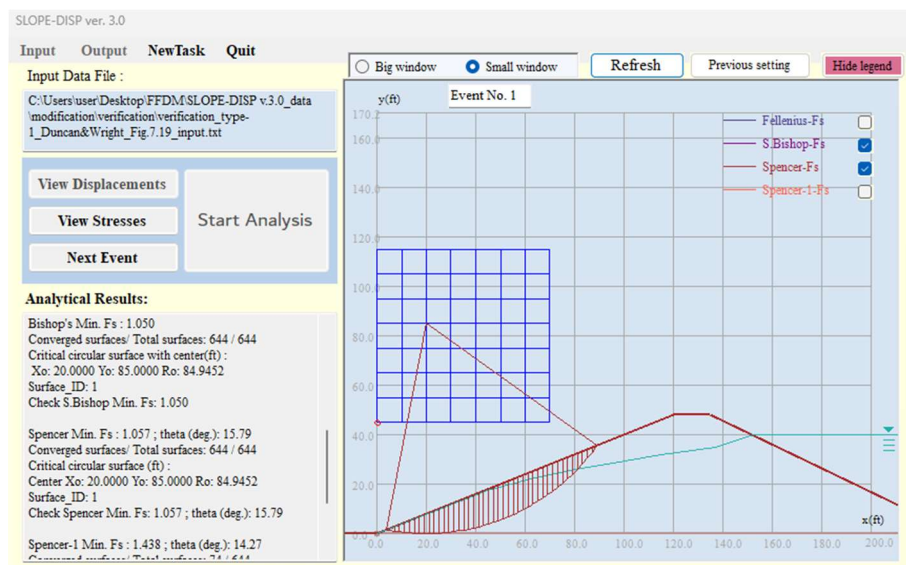


Figure 3.7.1 Critical circular surface obtained using Type-1 analysis with a presence of a piezometric line.

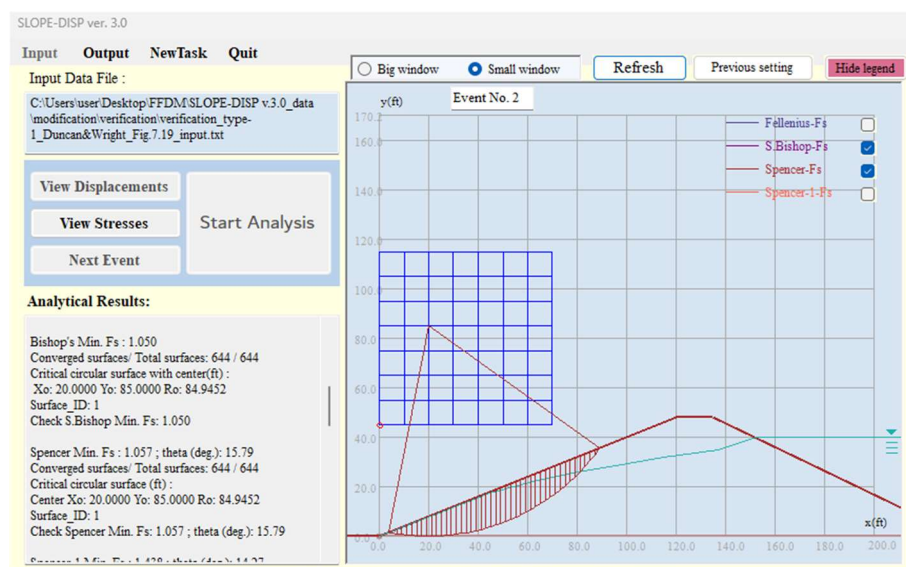


Figure 3.7.2 Critical circular surface obtained using Type-1 analysis with a presence of a phreatic surface.

REFERENCE

Huang, C.-C., Lo, C.-L., Jang, J.-S. and Hwu, L.-K. (2008) "Internal soil moisture response to rainfall-induced slope failures and debris discharge" Engineering Geology, 101, 134-145.

3.8 VERIFICATION CASE STUDY NO. 8

Input and output files for case study No. 8:

Input file name: verification_type-1_Duncan&Wright_Fig.7.26_input.txt

Output file name: verification_type-1_Duncan&Wright_Fig.7.26_output.txt

This is a hypothetical reinforced embankment on a clayey foundation. A geosynthetic reinforcement sheet is placed at the bottom of a 6 m-high embankment consisting of a cohesionless soil (Soil 1 in this study, Table 3.8.1). The foundation consists of 4 layers of clayey soils with varied undrained shear strength (c_u) expressed in Eq. 3-8-1. The input soil parameters are summarized in Table 3.8.1.

$$c_u = c_{u0} + \Delta c_u \times z \quad (3-8-1)$$

z : Depth from the top of soil layers

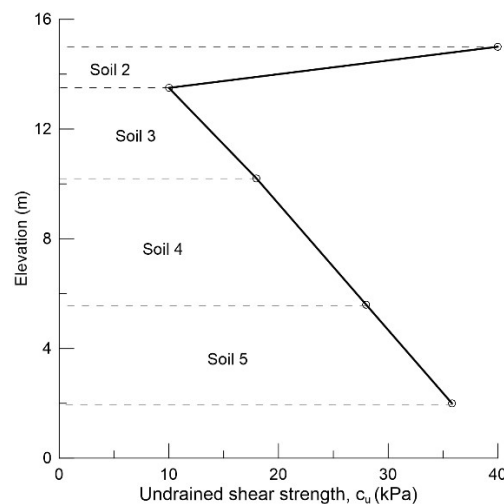


Figure 3.8.1 A clayey foundation with a varied undrained shear strength along depths

Table 3.8.1 Input soil strength parameters for the studied case

Soil layer No.	Elevation (m)	γ (kN/m ³)	ϕ (°)	C_{u0} (kPa)	ΔC_u (kPa/m)
1	15.0- 21.0	18.9	44.0	0	0
2	13.5- 15.0	18.4	0	40.0	-20.0
3	10.2- 13.5	16.0	0	10.0	2.42
4	5.6- 10.2	17.0	0	18.0	2.17
5	2.0- 5.6	19.2	0	28.0	2.17
6	1.0- 2.0	19.2	40	50.0	0

Duncan and Wright (2005) reported $F_s = 1.13- 1.19$ using two computer programs (STABGM and UTEXAS4) with an unknown value of input allowable tensile strength of reinforcement ($T_{allowable}$). Therefore, results of analyses using SLOPE-ffdm 2.0 as summarized in Table 3.8.2 are not intended to make a direct comparison of F_s between the reported and the calculated. Results shown in Table 3.8.2 reveal the fact that minimum values of F_s are influenced by the input value of $T_{allowable}$. The differences of F_s between the Spencer's and Bishop's methods are 1.9- 5.9%.

Critical failure surfaces obtained using Spencer's and Bishop's methods are shown in Figs. 3.8.2, 3.8.3, and 3.8.4 for the cases of $T_{allowable} = 300, 200$ and 100 kN/m. It is interesting to note that the depth of critical surfaces tends to decrease (or becomes shallower) as the input value of $T_{allowable}$ decreases.

Table 3.8.2 Safety factors for a reinforced embankment based on various input tensile strengths of reinforcement.

$T_{allowable}$ (kN/m)	F_s (Spencer's method)	F_s (Bishop's method)
300	1.541	1.478
200	1.298	1.225
100	1.036	1.034

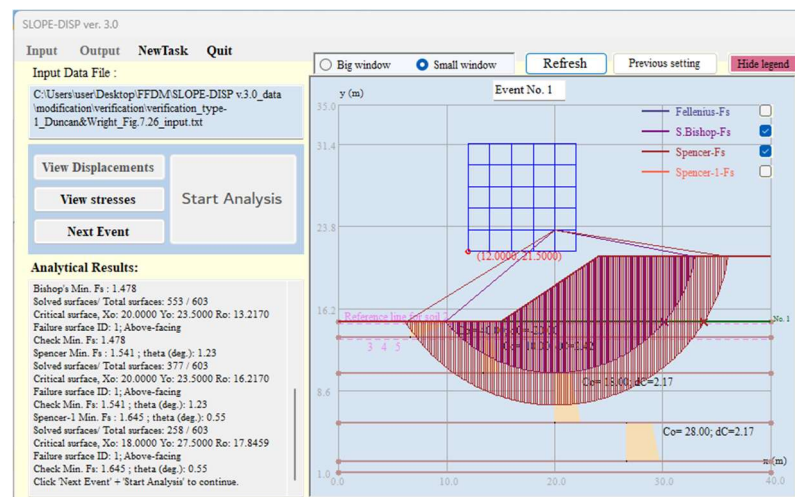


Figure 3.8.2 Critical circular surfaces obtained using Bishop's and Spencer's methods for the case of $T_{allowable} = 300$ kN/m

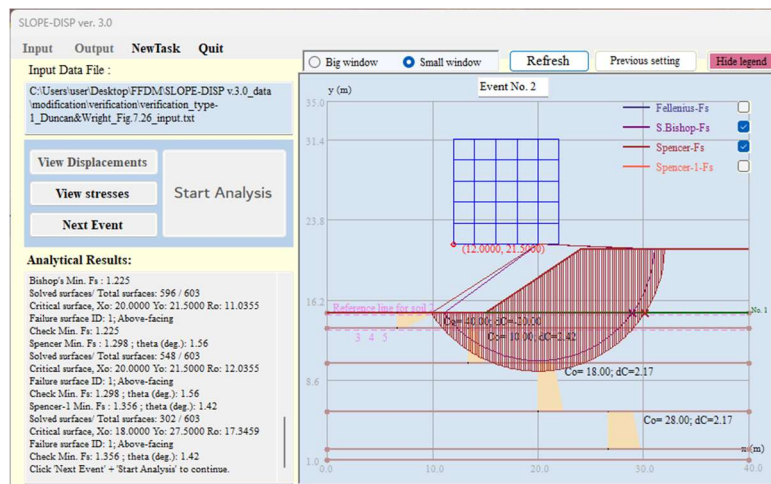


Figure 3.8.3 Critical circular surfaces obtained using Bishop's and Spencer's methods for the case of $T_{\text{allowable}} = 200 \text{ kN/m}$

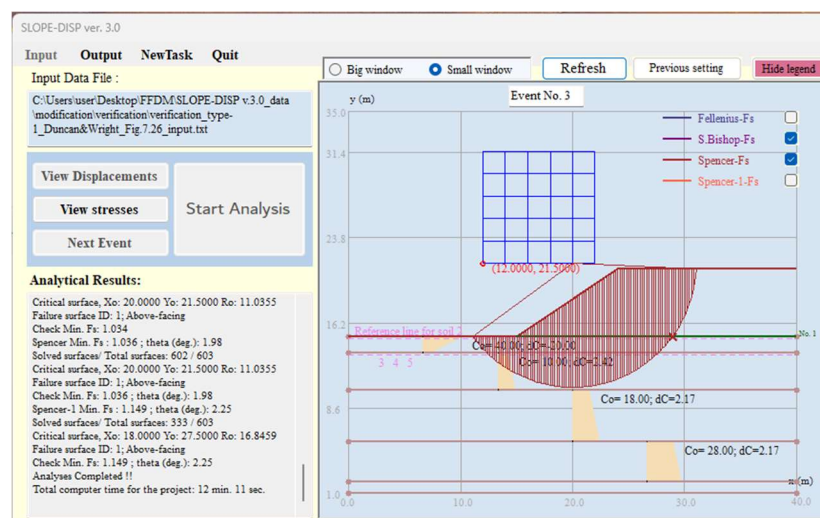


Figure 3.8.4 Critical circular surfaces obtained using Bishop's and Spencer's methods for the case of $T_{\text{allowable}} = 100 \text{ kN/m}$

REFERENCE

Duncan, J.M., Low, B.K., Schaefer, V.R., and Bentler, D.J. (1998) STABGM 2.0- A computer Program for Slope Stability Analysis of Reinforced and Unreinforced Embankments and Slopes. Department of Civil Engineering, Virginia Polytechnic Institute and State University, Blacksburg, VA.

3.9 VERIFICATION CASE STUDY NO. 9

Input and output files for case study No. 9:

Input file name: verification_type-1_Duncan&Wright_Fig.7.28_input.txt

Output file name: verification_type-1_Duncan&Wright_Fig.7.28_output.txt

This case is a hypothetical 24 ft-high reinforced slope backfilled with a cohesionless soil with $c=0$ and $\phi=37^\circ$. A total of five layer of reinforcement with an allowable tensile strength ($T_{allowable}$) of 800 lb/ft. The soil-reinforcement interface adherence is assumed zero, and an interface friction angle of $0.8\phi (=30^\circ)$. Based on a search from a total of 1994 trial-and-error circles, the minimum values of F_s are shown in Table 3.9.1 and the geometry of critical circle is shown in Fig. 3.9.1. The values of F_s and the geometry of critical arcs obtained in SLOPE-ffdm 2.0 are comparable with those reported in the literature. It is interesting to note that a large reduction of the interface friction angle to 0.3ϕ (implemented in Event 2 of the analysis) does not change the values of F_s , suggesting that the stability of this slope is not prone to the change of reinforcement-soil interface friction angles. The symbol "x" appeared in Fig. 3.9.1 represents a 'tiebreak' failure mode of reinforcement.

Table 3.9.1 Comparisons of minimum values of F_s obtained in various studies.

	Duncan and Wright (2005)	SLOPE-ffdm 2.0
F_s (Spencer's method)	1.61- 1.71	1.625
F_s (Bishop's method)	---	1.632

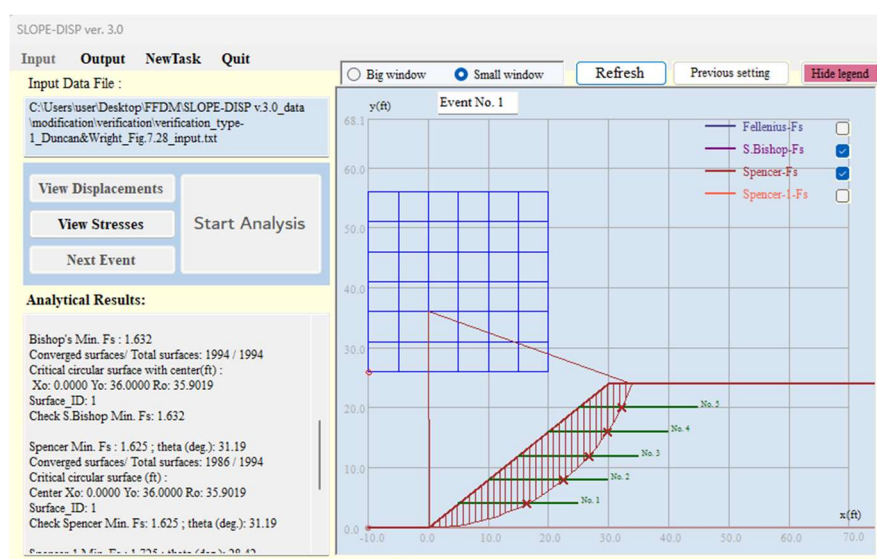


Figure 3.9.1 Critical circular surface for the studied reinforced slope

3.10 VERIFICATION CASE STUDY NO. 10

Input and output files for case study No. 10:

Input file name: verification_type-7_Leshchinsky&Huang1992_Fig.6_input.txt
Output file name: verification_type-7_Leshchinsky&Huang1992_Fig.6_output.txt

This is a case study reported by Chen and Shao (1988) and was re-visited by Leshchinsky and Huang (1992). A deep-seated failure along a weak seam with $c=9.8$ kPa, $\phi=16^\circ$. In the above-mentioned studies, straight lines were used as slip surfaces to describe the failure zone. A slightly different approach is used in the SLOPE-DISP analysis, i.e., using circular slip lines to replace the straight lines over the weak seam. This approach is based on the observation that a deep-seated failure in cohesive soils is usually curved, rather than straight ones. Table 3.10.1 supports the use of compound failure surfaces to describe the failure of this slope, i.e., $F_s=0.999$ by the rigorous Janbu's method which is marginally smaller than that reported by Chen and Shao (1988), and $F_s=1.059$ by using Spencer's method which is comparable to $F_s=1.061-1.066$ obtained by variational calculus method.

Table 3.10.1 Comparisons of F_s obtained using various methods.

	Chen and Shao (1988)	Leshchinsky and Huang (1992)	SLOPE-ffdm 2.0 (Event 1)
Morgenstern-Price	1.010	--	--
Variational Calculus	--	1.061- 1.066	--
Rigorous Janbu	--	1.029	0.994
Spencer	--	--	1.048

Table 3.10.2 Results of parametric study on the configurations of weak seam using Type-1 analysis of SLOPE-ffdm 2.0.

	Weak seam with gentle slope and concave down (Event 1; Fig. 3.10.1)	Weak seam with gentle slope and concave upward (Event 2; Fig. 3.10.2)
Rigorous Janbu	0.999	0.793
Spencer	1.048	0.893

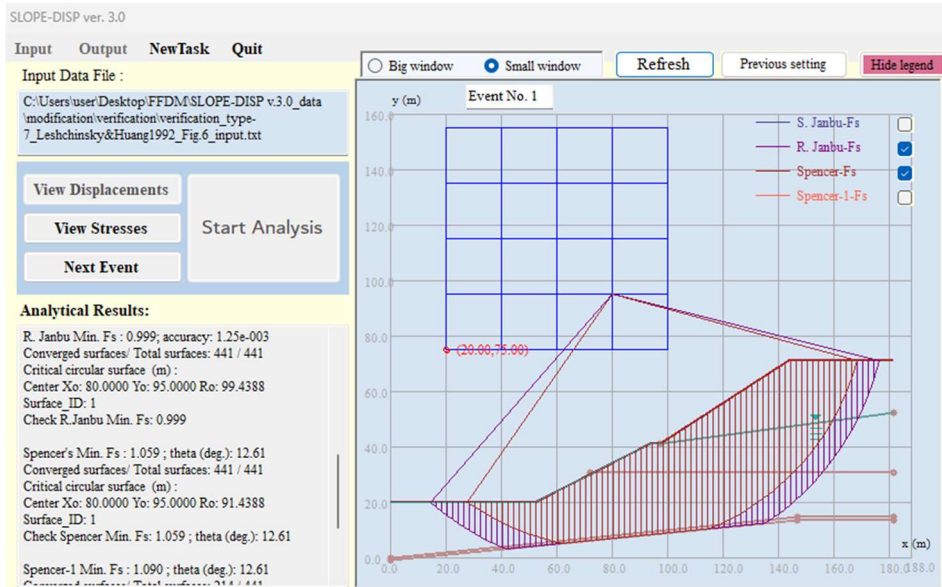


Figure 3.10.1 Critical compound surfaces obtained in SLOPE-ffdm 2.0 analysis

Note that the weak seam in Fig. 3.10.1 is a concave down polyline with gentle slopes. A hypothetical case of a concave up weak seam with a steeper slope is analyzed as Event 2 of analysis to verify the compound surface generation procedure and the analytical results. The resulted values of F_s in comparison with those reported earlier is summarized in Table 3.10.2. The significant influence of the configuration of weak seam can be detected in Table 3.10.2. The critical surfaces shown in Fig. 3.10.2 also reveal the effectiveness of SLOPE-ffdm 2.0 in processing weak seams with complex configurations.

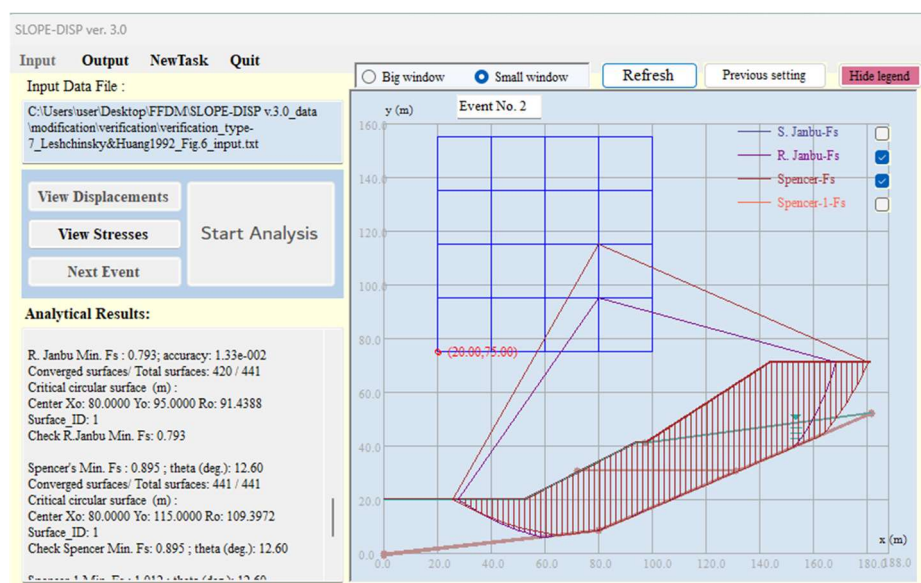


Figure 3.10.2 Critical compound surface in Event 2 analysis for the slope with a

concave-upward weak seam.

REFERENCE

Chen, Z.-Y. and Shao, C.-M. (1988) "Evaluation of minimum factor of safety in slope stability analysis." *Canadian Geotechnical Journal*, Vol. 25, No. 4, pp. 735-748.

Leshchinsky, D. and Huang, C.-C. (1992) "Generalized slope stability analysis: Interpretation, Modification, and Comparison" *Journal of Geotechnical Engineering*, Vol. 118, No. 10, pp. 1559- 1576.

3.11 VERIFICATION CASE STUDY NO. 11

Input and output files for Type-6B analysis of case No. 11:

Input file name: verification_type-6B_Leshchinsky&Huang1992_Fig.7_input.txt
Output file name: verification_type-6B_Leshchinsky&Huang1992_Fig.7_output.txt

Input and output files for Type-5 analysis of case No. 11:

Input file name: verification_type-5_Leshchinsky&Huang1992_Fig.7_input.txt
Output file name: verification_type-5_Leshchinsky&Huang1992_Fig.7_output.txt

This is a case study reported by Chen and Shao (1988) and was later revisited by Leshchinsky and Huang (1992). The multi-layer natural slope subjected to a landslide failure, having an apparent failure surface as shown in Fig. 3.11.1. A Type-6B analysis (for a specific non-circular failure surface described using a polyline) is performed using SLOPE-ffdm 2.0. Calculated values of F_s are compared with those reported in the literature in Table 3.11.1. Results of Type-6B analysis indicate that the value of $F_s=0.794$ obtained using the rigorous Janbu's method is deviated from that reported ($F_s=0.863$) by Leshchinsky and Huang (1992) by 8%. In general, the values of F_s obtained here are 8-13% smaller than those reported by Leshchinsky and Huang (1992) by using various methodologies.

Table 3.11.1 Comparisons of F_s for the apparent slip surface reported by Chen and Shao (1988)

	Chen and Shao (1988)	Leshchinsky and Huang (1992)	SLOPE-ffdm 2.0 (Type-6B analysis)
Morgenstern-Price	0.917	--	--
Variational Calculus	--	0.876 - 0.889	--
Rigorous Janbu	--	0.863	0.851
Spencer	--	--	0.812

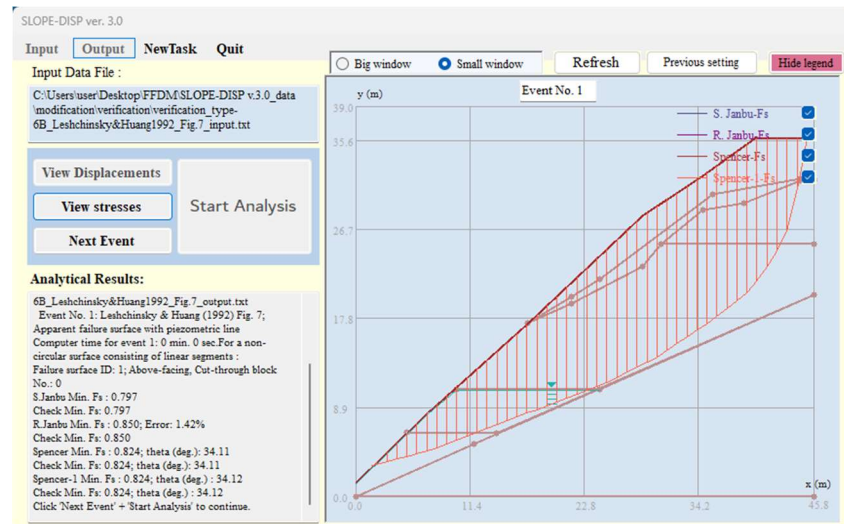


Figure 3.11.1 Results of Type-6B analysis for the apparent failure surface reported by Chen and Shao (1988).

A trial-and-error search for the critical surface and a minimum value of F_s is performed as the event 1 of Type-5 analysis (trial-and-error search using logarithmic spiral surfaces without tension crack). The critical surface found in the analysis is shown in Figs. 3.11.2. A unique critical surface is found, regardless of the method used. The associated minimum values of F_s are shown in Table 3.11.2. The minimum values of F_s found in the trial-and-error search are 4- 7 % smaller than those obtained in the Type-6B analysis (Table 3.11.1) for the apparent failure surface reported by Chen and Shao (1988). Although the failure mechanism used in Type-5 analysis may be different from that reported by Chen and Shao (1988) which has a close-to-vertical slip surface at the crest, the trial-and-error search using logarithmic failure mechanism is considered as an effective tool in addition to the circular failure used in Type-1, 2 and 3 analyses.

To investigate the influence of tension cracks on the results of slope stability, Event 2 of Type-5 analysis is performed. Introducing a 2.5m-deep tension crack resulted in 2% lower F_s compared with those without tension crack. Although, this variation of F_s seems small, introducing a tension crack at the crest of slope may improve the situation of unacceptable effective normal stresses at slice base and inter-slice thrusts, as demonstrated in Figs. 3.11.4 through 3.11.7.

Table 3.11.2 Influence of tension cracks on F_s obtained in trial-and-error logarithmic surface search (Type-5 analysis)

	Type-5 analysis (no tension crack)	Type-5 analysis (with tension crack)
Rigorous Janbu	0.779	0.758
Spencer	0.776	0.755

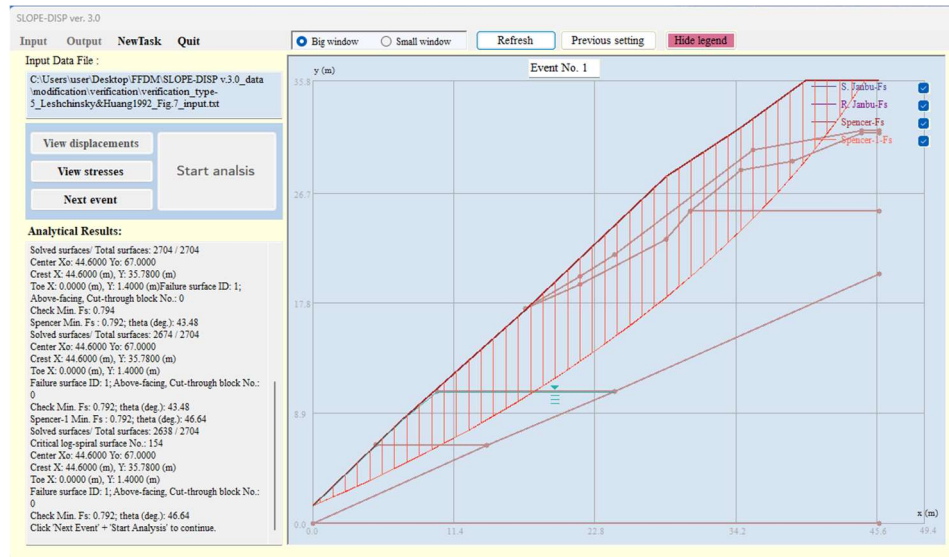


Figure 3.11.2 Critical surface found in Event 1 of Type-5 analysis (trial-and-error search using logarithmic spiral surfaces without tension crack)

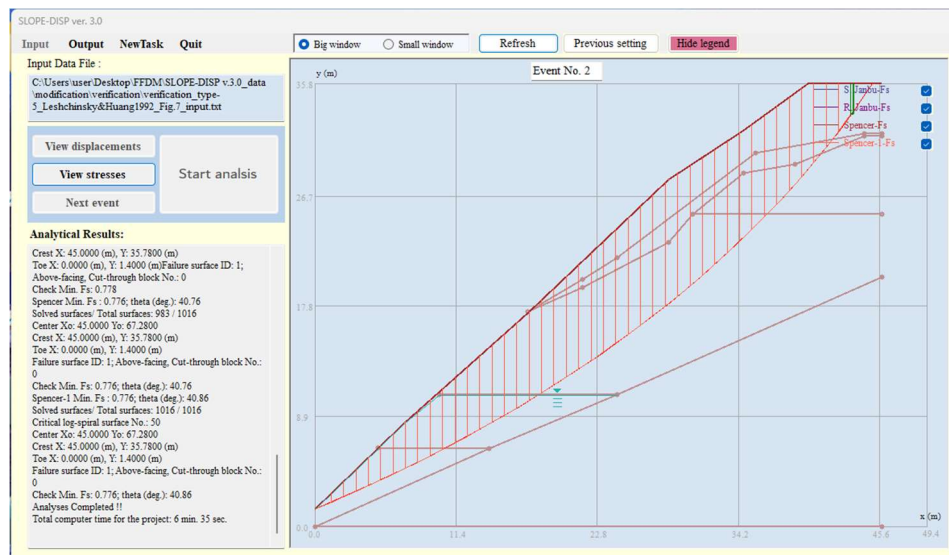


Figure 3.11.3 Critical surface found in Event 2 of Type-5 analysis (trial-and-error search using logarithmic spiral surfaces with a 2.5m-deep tension crack)

Figures 3.11.4 and 3.11.5 show the case without tension crack for Spencer and R. Janbu, respectively. In this case, the Spencer method generates an acceptable distribution of effective normal stresses at slice base but failed to obtain an acceptable distribution of inter-slice thrusts. On the other hand, the R. Janbu method has unacceptable negative values of normal stress at slice base (slice No. 1, 2 from the crest) and inter-slice thrust (left sides of slice Nos. 1- 4). These unacceptable conditions can be partially improved by introducing a 2.5m-deep tension crack at the crest, as shown in Figs. 3.11.6- 3.11.7. This example highlights the fact that the fundamental assumptions of $f(x)=1.0$ in Spencer method and the point of inter-slice thrust at 1/3 height of inter-slice face not always give acceptable solutions in terms of slice base normal stress distributions and inter-slice thrusts. For slope stability problems with specific boundary and soil conditions, a cross check with multiple methods is a good way to a successful analysis.

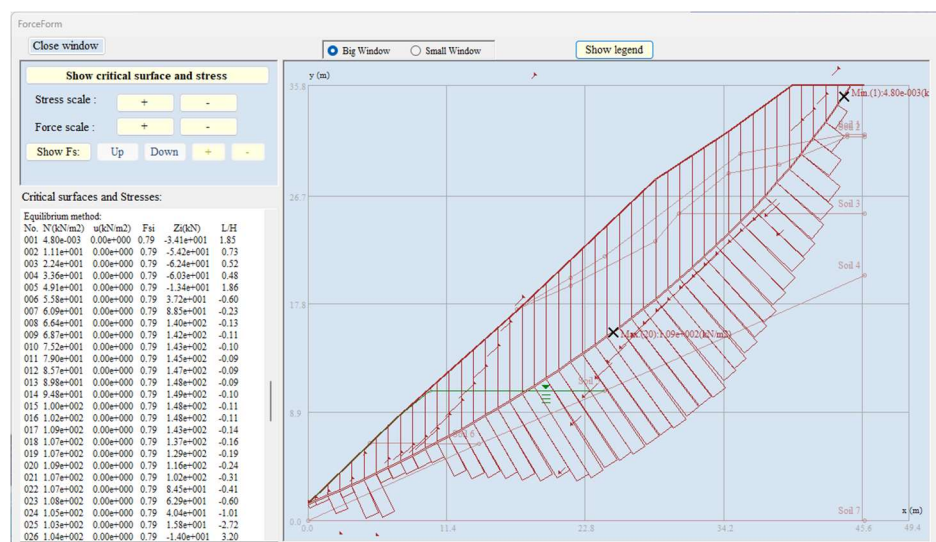


Figure 3.11.4 Effective normal stress at slice base and inter-slice thrust for the critical surface in Spencer method (Event 1, no tension crack)

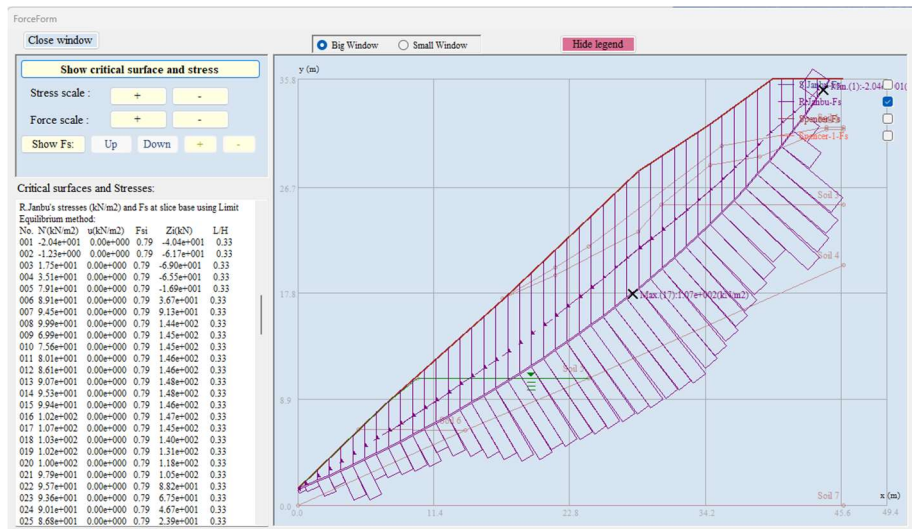


Figure 3.11.5 Effective normal stress at slice base and inter-slice thrust for the critical surface in rigorous Janbu method (Event 1, no tension crack)

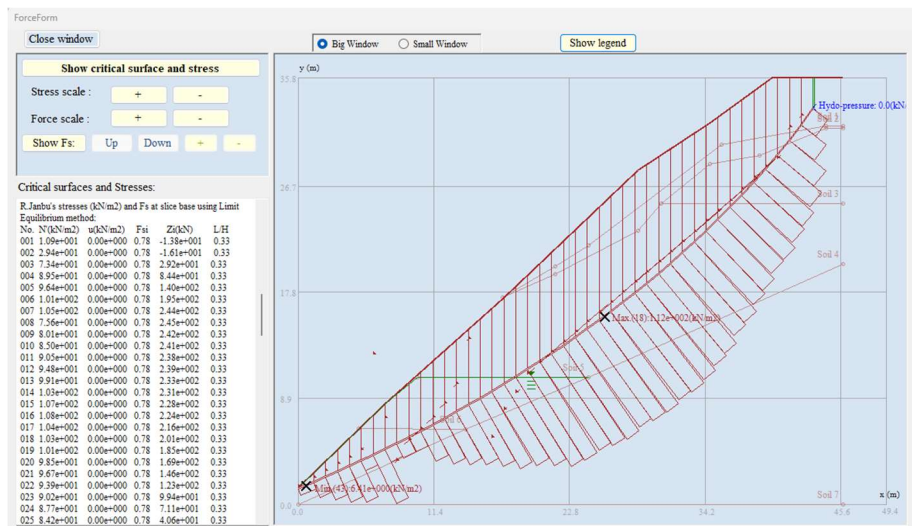


Figure 3-11-6 Effective normal stress at slice base and inter-slice thrust for the critical surface in Spencer method (Event 2, with a 2.5m-deep tension crack)

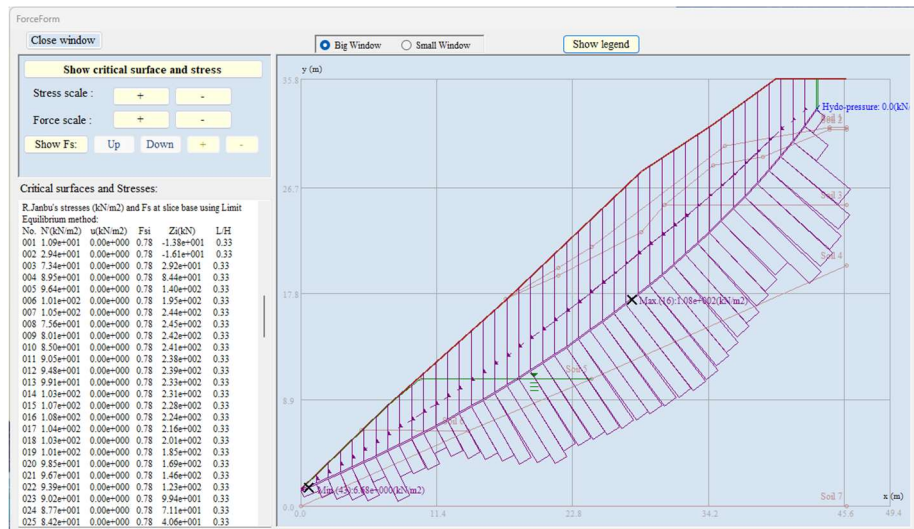


Figure 3-11-7 Effective normal stress at slice base and inter-slice thrust for the critical surface in rigorous Janbu method (Event 2, with a 2.5m-deep tension crack)

REFERENCE

- Chen, Z.-Y. and Shao, C.-M. (1988) "Evaluation of minimum factor of safety in slope stability analysis." Canadian Geotechnical Journal, Vol. 25, No. 4, pp. 735-748.
- Leshchinsky, D. and Huang, C.-C. (1992) "Generalized slope stability analysis: Interpretation, Modification, and Comparison" Journal of Geotechnical Engineering, Vol. 118, No. 10, pp. 1559- 1576.

3.12 VERIFICATION CASE STUDY NO. 12

Input and output files for case study No. 12:

Input file name: verification_type-8_Leshchinsky&Huang1992_Fig.8_input.txt
Output file name: verification_type-8_Leshchinsky&Huang1992_Fig.8_output.txt

This is a 12 m-high, 2:1 (H: V) slope with a known circular (or compound) slip surface with a rotation center at (x= 12.7 m, y= 27.4 m) and a radius of R= 24.4 m. Stability analyses were performed for the slip surface under six groundwater and geological conditions:

Case 1: Homogeneous slope with $\gamma = 18.84 \text{ kN/m}^3$, $\phi' = 20^\circ$, $c = 28.7 \text{ kPa}$.

Case 2: Same as Case 1, except with a weak seam ($c' = 0$, $\phi = 10^\circ$).

Case 3: Same as Case 1, except with $r_u = 0.25$ (r_u : pore pressure ratio, see details in Section 2.5).

Case 4: Same as Case 2, except with $r_u = 0.25$.

Case 5: Same as Case 1, except with a piezometric line.

Case 6: Same as Case 2, except with a piezometric line.

In the study using SLOPE-ffdm 2.0, the above Case 1- 6 are analyzed using Event 1 – 6 in the input data file. The results are summarized in Table 3.12.1. Comparisons of F_s obtained by the Morgenstern-Price and those by the Spencer method reveal that the differences are less than 1.8%. Comparisons of F_s obtained using R. Janbu's in SLOPE-ffdm 2.0 are comparable to those reported by Leshchinsky and Huang (1992) using R. Janbu's and variational calculus methods with differences between -4% ~ +6%, only with one exception of Case 6 for which $F_s = 1.182$ obtained here is about 9% smaller than $F_s = 1.298$ reported by Leshchinsky and Huang (1992).

Figures 3.12.1 and 3.12.2 shows results of Case 5 and Case 6, respectively, analyses. Fig. 3.12.1 highlights a special technique regarding the input data, i.e., to implement the Type-8 (or Type-7) analysis, it is necessary to incorporate a weak seam (or weak layer) in the slope profile. This seems contradictory to the geological condition of Case 5 in which a weak seam is non-existent. To clear this issue, a weak seam is intentionally located at a deep location out of the reach of all trial-and-error surfaces. Results of using this technique can be seen in Fig. 3.12.1 in which a weak layer of about 1 m-thick (the thickness can be arbitrarily chosen; in Fig. 3.12.2, a 0.1 m-thick weak seam is used) is incorporated.

Table 3.12.1 Comparisons of F_s obtained for Case 1- 6 reported by Fig. 8 of Leshchinsky and Huang (1992)

	Fredlund and Krahn (1977)	Leshchinsky and Huang (1992)		SLOPE-ffdm 2.0 (Type-8 analysis)	
	Morgenstern-Price Inter-slice function $f(x)=1$	R. Janbu	Variational Calculus	R. Janbu	Spencer
Case 1	2.076	2.008	2.053-2.080	2.195	2.104
Case 2	1.378	1.432	1.312-1.333	1.409	1.359
Case 3	1.765	1.708	1.739-1.765	1.861	1.784
Case 4	1.124	1.162	1.067-1.080	1.125	1.141
Case 5	1.833	1.776	1.813-1.839	1.931	1.843
Case 6	1.250	1.298	1.181-1.197	1.239	1.264

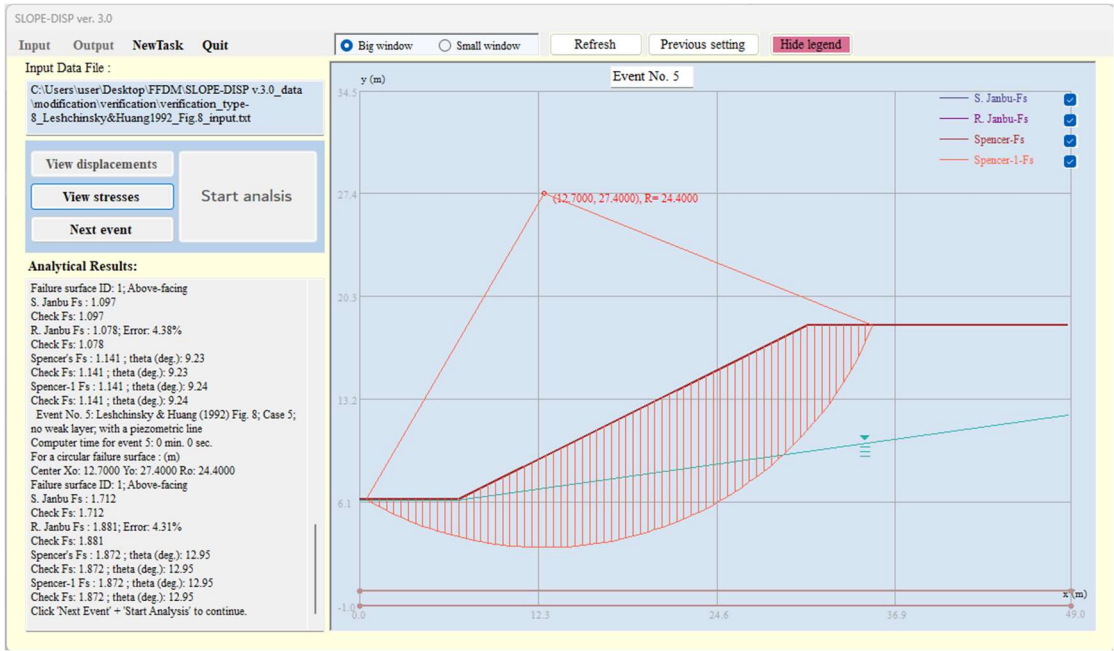


Figure 3.12.1 Results of Type-8 analysis for Case 5 of Fig. 8 reported by Leshchinsky and Huang (1992)

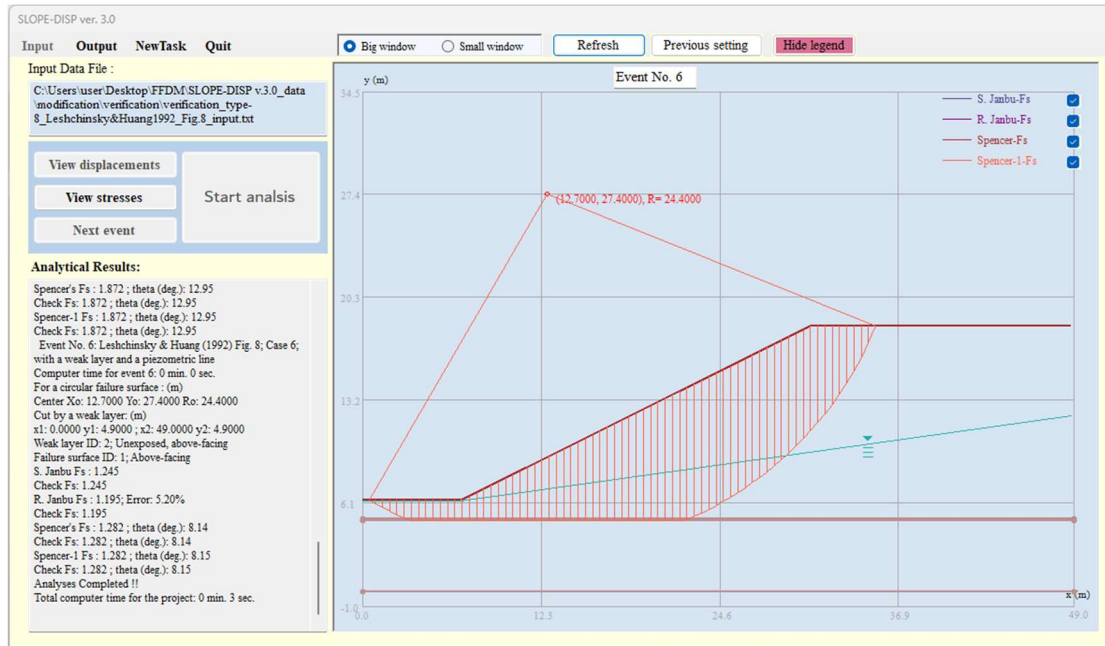


Figure 3.12.2 Results of Type-8 analysis for case 6 of Fig. 8 reported by Leshchinsky and Huang (1992)

The following generalized interslice function has been proposed by Spencer (1973) and Mogenstern and Price (1980??). In which, $f(x_i)$ can be an arbitrary function:

$$\tan \delta_i = f(x_i) \tan \theta \quad (3 - 12 - 1)$$

One of the following three types of $f(x)$ can be assigned by the users of SLOPE-ffdm 2.0:

Type-1: $f(x_i) = 1$; this is the default of the computer program, generating a constant inclination angle $\delta_i = \theta$ ($i = 1 \dots ns$) throughout the sliding mass, $0 \leq x_i \leq 1$ (x_i : normalized x-coord. of slice No. i).

Type-2: $f(x_i) = \sin(\pi x_i)$; this is a half-sine function; $0 \leq f(x_i) \leq 1$, $0 \leq x_i \leq 1$.

Type-3: $f(x_i)$ is defined by a polyline with a total number of points, n , and their coordinates (x_i, y_i) ; $0 \leq x_i \leq 1$ and $0 \leq y_i \leq 1$; x_i : the normalized x-coord.; y_i : inter-slice force function.

In general, the use of $f(x_i) = 1.0$ generates good results of F_s . Mogenstern and Price (1965) proposed the use of a half-Sine inter-slice function to obtain an acceptable result of slope stability analysis. Spencer (1973) has demonstrated the effectiveness of using various functions of $f(x_i)$ to improve the rationality of inter-slice thrust height

distributions. In the following analyses, the Type-2 inter-slice function defined as following is used:

$$f(x_i) = \sin \left[\pi \cdot \frac{(W - D_i)}{W} \right] \quad (3 - 12 - 2)$$

W: the full width of the slip surface

D_i : distance between slice No. i and the toe of the slip surface

Table 3.12.2 shows a comparison of the values of F_s between those reported by Fredlund and Krahn (1977) and SLOPE-ffdm 2.0 for Case 1- 6. The values of F_s obtained here are within a negligibly small range of $\pm 2\%$ compared to those reported by Fredlund and Krahn (1977).

Table 3.12.2 Comparisons of F_s obtained in different studies
with a half-Sine interslice function

	Fredlund and Krahn (1977)	SLOPE-ffdm 2.0 (Type-8 analysis)
Methods	Morgenstern-Price method	Spencer's method
Case 1	2.076	2.104
Case 2	1.370	1.350
Case 3	1.764	1.784
Case 4	1.118	1.129
Case 5	1.832	1.843
Case 6	1.245	1.255

REFERENCE

Chen, Z.-Y. and Shao, C.-M. (1988) "Evaluation of minimum factor of safety in slope stability analysis." Canadian Geotechnical Journal, Vol. 25, No. 4, pp. 735-748.

Fredlund, D.G. and Krahn, J. (1977) "Comparison of slope stability methods of analysis" Canadian Geotechnical Journal, Vol. 14, No. 3, pp. 429-439.

Leshchinsky, D. and Huang, C.-C. (1992) "Generalized slope stability analysis: Interpretation, Modification, and Comparison" Journal of Geotechnical Engineering, Vol. 118, No. 10, pp. 1559- 1576.

Morgenstern, N.R. and Price, V.E. (1965) "The analysis of stability of general slip surfaces" Geotechnique, Vol. 15, No.1, pp. 79-93.

3.13 VERIFICATION CASE STUDY NO. 13

Input and output files for case study No. 13:

Input file name: verification_type-8_spencer1973_ns=102_input.txt
Input file name: verification_type-8_spencer1973_ns=16_input.txt
Output file name: verification_type-8_spencer1973_ns=102_output.txt
Output file name: verification_type-8_spencer1973_ns=16_output.txt

This is a case study reported by Spencer (1973) on a homogeneous gentle slope consisting of a $c-\phi$ soil. In this study, the inter-slice force function, $k(x)$, the depth of tension crack (z_t), are varied to investigate their effects on the safety factor (F_s), the value of $\tan \theta$, the inter-slice force (Z_i), and the height of normal component of inter-slice force from the bottom of slices (L_i). Table 14-14 compares values of F_s and $\tan \theta$ reported by Spencer (1973) and those obtained by SLOPE-ffdm 2.0.

Table 3.13.1 shows that SLOPE-ffdm 2.0 generates more responsive outputs of F_s and $\tan \theta$ than those reported by Spencer (1973) with the changes of tension crack depths and the types of interslice function $k(x)$. The author believes that the differences between those reported by Spencer (1973) and those obtained here reflect the difference of computational technologies in different eras. In general, SLOPE-ffdm 2.0 generates more responsive outputs of F_s and $\tan \theta$ than those reported by Spencer (1973) with the changes of tension crack depths and the types of interslice function $k(x)$. Accuracy of formulas described here and the computer program SLOPE-ffdm 2.0 is verified.

Table 3.13.1 Comparisons of F_s and $\tan \theta$ obtained in various studies

Input conditions			Spencer(1973) $ns = 16$		SLOPE-ffdm 2.0 $ns = 16$		SLOPE-ffdm 2.0 $ns = 102$	
Event	z/H_t	$k(x)$ type	F_s	$\tan \theta$	F_s	$\tan \theta$	F_s	$\tan \theta$
1	0	1	1.46	0.26	1.462	0.253	1.462	0.255
2	0.1	1	1.46	0.26	1.450	0.252	1.453	0.258
3	0.2	1	1.46	0.26	1.446	0.249	1.450	0.259
4	0.3	1	1.46	0.26	1.448	0.246	1.455	0.259
5	0.2	2	1.46	0.27	1.444	0.255	1.451	0.270
6	0.2	3	1.46	0.36	1.447	0.346	1.454	0.368

Figure 3.13.1 shows the slope and slices ($ns=16$) used in the analysis of Event 3. The use of $ns=16$ is to comply with that reported by Spencer (1973). The result of stress

analysis for this event is shown in Figure 3.13.1. Some points of lateral thrust application near to the crest of the slope seem to fall below the slip surface. On the other hand, in the case of $ns=102$ as shown in Figs. 3.13.3 and 3.13.4, the points of lateral thrust application are close to 1/3 of the side-face of the slice. This improvement in the point of thrust calculations is attributable to the increased accuracy in some simplified terms of the moment equilibrium formulations.

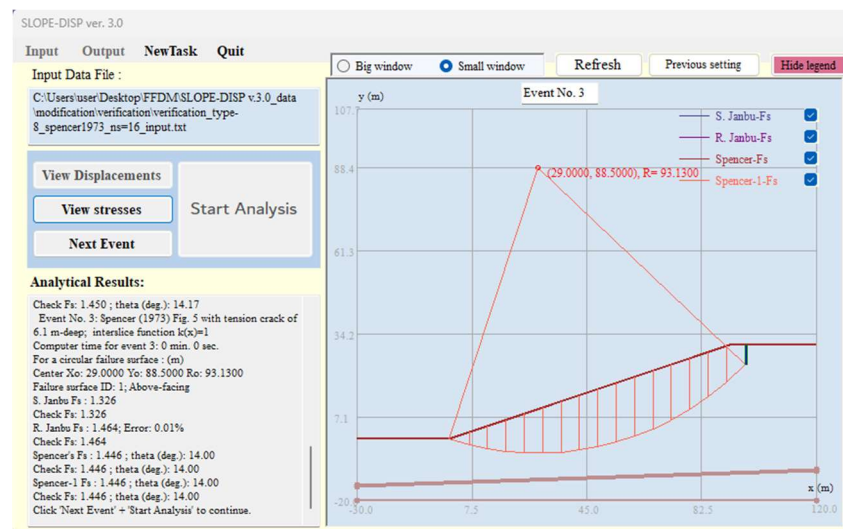


Figure 3.13.1 Results of Event 3 analysis using $ns=16$ in SLOPE-ffdm 2.0 for the slope reported by Spencer (1973).

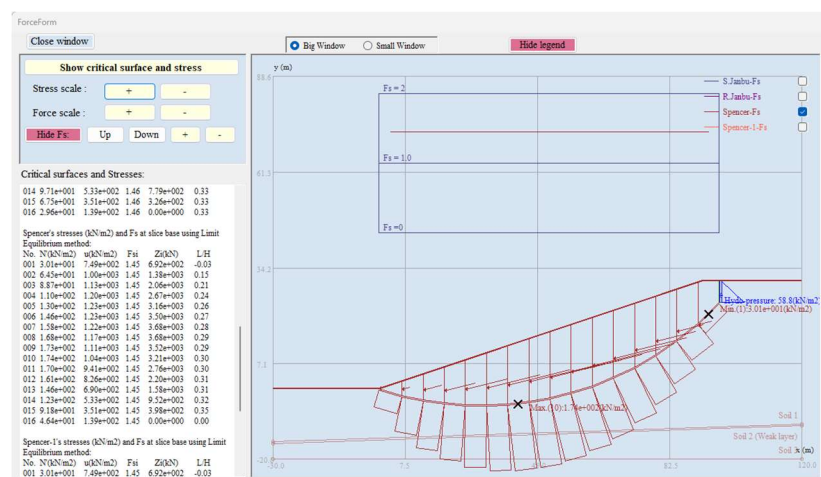


Figure 3.13.2 Results of stress analysis for Event 3 analysis using $ns=16$ in SLOPE-ffdm 2.0 for the slope reported by Spencer (1973).

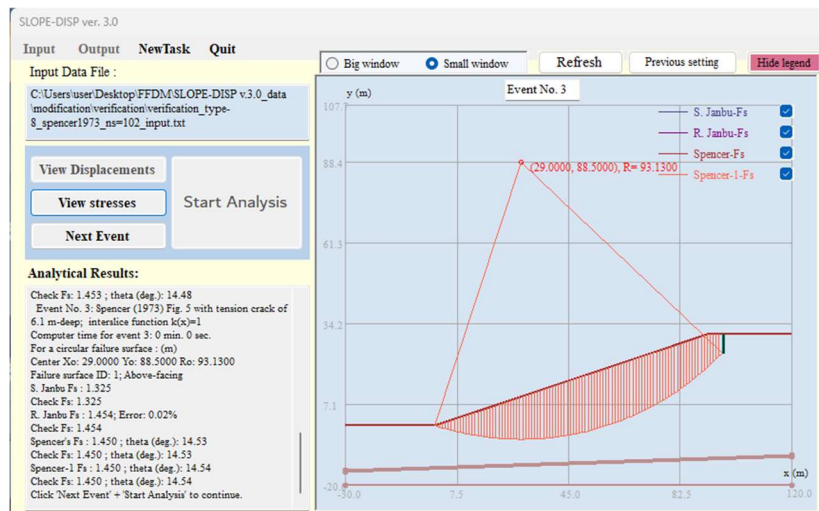


Figure 3.13.3 Results of Event 3 analysis using $ns=102$ in SLOPE-ffdm 2.0 for the slope reported by Spencer (1973).

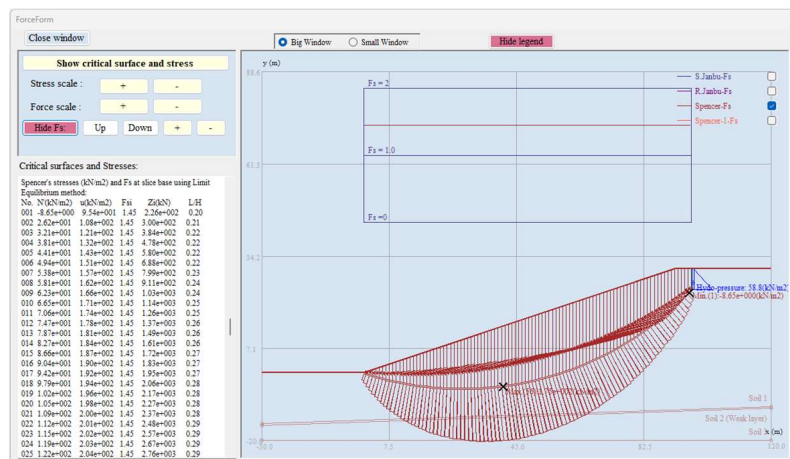


Figure 3.13.4 Results of stress analysis for Event 3 analysis using $ns=102$ in SLOPE-ffdm 2.0 for the slope reported by Spencer (1973).

Other than F_s and the value of $\tan \theta$, the Effective normal stress (N_i'), porewater pressure acting on the slice base (U_i), inter-slice total force (Z_i), inter-slice effective normal force ($Z_i' \cos \delta_i$), the inter-slice total thrust height ratio (h_i/H_i), and the inter-slice effect normal force height ratio (h_i'/H_i) are included in the output data file. As a default in SLOPE-ffdm 2.0, in addition to the Spencer's method, simplified Janbu's and the rigorous Janbu's methods are also used to analyze the same slope with identical input conditions as those used in the slope reported by Spencer (1973).

REFERENCES

Spencer, E. (1973). Thrust line criterion in embankment stability analysis. *Geotechnique*, 23, No. 1, 85-100.